NASA/TP-2005-213945

Cross Section Sensitivity and Propagated Errors in HZE Exposures

John H. Heinbockel
Old Dominion University, Norfolk, Virginia

John W. Wilson, Steve R. Blattnig, and Garry D. Qualls
NASA Langley Research Center, Hampton, Virginia

Francis F. Badavi
Christopher Newport University, Newport News, Virginia

Francis A. Cucinotta
NASA Johnson Space Center, Houston, Texas

December 2005

The NASA STI Program Office . . . in Profile

Since its founding, NASA has been dedicated to the advancement of aeronautics and space science. The NASA Scientific and Technical Information (STI) Program Office plays a key part in helping NASA maintain this important role.

The NASA STI Program Office is operated by Langley Research Center, the lead center for NASA's scientific and technical information. The NASA STI Program Office provides access to the NASA STI Database, the largest collection of aeronautical and space science STI in the world. The Program Office is also NASA's institutional mechanism for disseminating the results of its research and development activities. These results are published by NASA in the NASA STI Report Series, which includes the following report types:

- TECHNICAL PUBLICATION. Reports of completed research or a major significant phase of research that present the results of NASA programs and include extensive data or theoretical analysis. Includes compilations of significant scientific and technical data and information deemed to be of continuing reference value. NASA counterpart of peer-reviewed formal professional papers, but having less stringent limitations on manuscript length and extent of graphic presentations.

- TECHNICAL MEMORANDUM. Scientific and technical findings that are preliminary or of specialized interest, e.g., quick release reports, working papers, and bibliographies that contain minimal annotation. Does not contain extensive analysis.

- CONTRACTOR REPORT. Scientific and technical findings by NASA-sponsored contractors and grantees.

- CONFERENCE PUBLICATION. Collected papers from scientific and technical conferences, symposia, seminars, or other meetings sponsored or co-sponsored by NASA.

- SPECIAL PUBLICATION. Scientific, technical, or historical information from NASA programs, projects, and missions, often concerned with subjects having substantial public interest.

- TECHNICAL TRANSLATION. English-language translations of foreign scientific and technical material pertinent to NASA's mission.

Specialized services that complement the STI Program Office's diverse offerings include creating custom thesauri, building customized databases, organizing and publishing research results ... even providing videos.

For more information about the NASA STI Program Office, see the following:

- Access the NASA STI Program Home Page at ***http://www.sti.nasa.gov***

- E-mail your question via the Internet to help@sti.nasa.gov

- Fax your question to the NASA STI Help Desk at (301) 621-0134

- Phone the NASA STI Help Desk at (301) 621-0390

- Write to:
  NASA STI Help Desk
  NASA Center for AeroSpace Information
  7121 Standard Drive
  Hanover, MD 21076-1320

NASA/TP-2005-213945

Cross Section Sensitivity and Propagated Errors in HZE Exposures

John H. Heinbockel
Old Dominion University, Norfolk, Virginia

John W. Wilson, Steve R. Blattnig, and Garry D. Qualls
NASA Langley Research Center, Hampton, Virginia

Francis F. Badavi
Christopher Newport University, Newport News, Virginia

Francis A. Cucinotta
NASA Johnson Space Center, Houston, Texas

National Aeronautics and
Space Administration

Langley Research Center
Hampton, Virginia 23681-2199

December 2005

Available from:

NASA Center for AeroSpace Information (CASI)
7121 Standard Drive
Hanover, MD 21076-1320
(301) 621-0390

National Technical Information Service (NTIS)
5285 Port Royal Road
Springfield, VA 22161-2171
(703) 605-6000

ABSTRACT

It has long been recognized that galactic cosmic rays are of such high energy that they tend to pass through available shielding materials resulting in exposure of astronauts and equipment within space vehicles and habitats. Any protection provided by shielding materials result not so much from stopping such particles but by changing their physical character in interaction with shielding material nuclei forming, hopefully, less dangerous species. Clearly, the fidelity of the nuclear cross-sections is essential to correct specification of shield design and sensitivity to cross-section error is important in guiding experimental validation of cross-section models and database. We examine the Boltzmann transport equation which is used to calculate dose equivalent during solar minimum, with units (cSv/yr), associated with various depths of shielding materials. The dose equivalent is a weighted sum of contributions from neutrons, protons, light ions, medium ions and heavy ions. We investigate the sensitivity of dose equivalent calculations due to errors in nuclear fragmentation cross-sections. We do this error analysis for all possible projectile-fragment combinations (14,365 such combinations) to estimate the sensitivity of the shielding calculations to errors in the nuclear fragmentation cross-sections. Numerical differentiation with respect to the cross-sections will be evaluated in a broad class of materials including polyethylene, aluminum and copper. We will identify the most important cross-sections for further experimental study and evaluate their impact on propagated errors in shielding estimates.

Introduction

Particle transport equations are derived from continuum mechanics principles, (Wilson et al 1991). The particle flux in a shielding material is determined by balancing the change in particle flux across a small volume element of material with gains and losses caused by atomic and nuclear collisions within the material. The resulting equation is the well known Boltzmann equation in the continuous slowing down approximation given as

$$[\Omega \bullet \nabla - \frac{1}{A_j}\frac{\partial}{\partial E} S_j(E) + \sigma_j(E)]\phi_j(x,\Omega,E) = \sum_k \int_E \int_\Omega dE'\, d\Omega' \sigma_{jk}(E,E',\Omega,\Omega')\phi_k(x,\Omega',E') \qquad (1)$$

where $\phi_j(x,\Omega,E)$ represents the flux of type j-particles with atomic mass A_j at position x with motion in the direction Ω having energy E. Occurring in the equation (1) are the terms $\sigma_j(E)$ which represents the macroscopic cross section, $S_j(E)$ representing the linear energy transfer or change in energy per unit distance. The fragmentation of the projectile and target nuclei is represented by the fragmentation cross sections $\sigma_{jk}(E,E',\Omega,\Omega')$ which represents the production cross section for type j particles with energy E

and direction Ω having a collision with a type k particle of energy *E'* with direction Ω'. That is, σ_{jk} is a cross-section for producing ion j from a collision by ion k. These cross sections are composed of three parts and can be written

$$\sigma_{jk}(E,E',\Omega.,\Omega') = \sigma_k(E')\upsilon_{jk}(E')\ f_{jk}(E,E',\Omega,\Omega') \qquad (2)$$

where $\upsilon_{jk}(E')$ represents the average number of type j particles produced by a collision with a type k particle of energy *E'*. The term $f_{jk}(E,E',\Omega,\Omega')$ is the probability density distribution for producing particles of type j of energy *E* into the direction Ω from the collision of the type k particle with energy *E'* moving in the direction Ω'. See Wilson, et al 1991.

The propagation of galactic cosmic rays into shielding material (Cucinotta, et al 2003) is described by the above Boltzmann equation. The galactic cosmic ray (GCR) transport radiation code HZETRN, (Shin et al 1992), was developed by NASA Langley Research Center around the 1980-1990 period. This code solves a one-dimensional form of the equation (1) and uses quality factors (ICRP, 1991) to calculate total radiation dose equivalent, in units of cSv/yr at various depths in a shielding material. The results are particularly important in determining radiation exposure of astronauts and electrical equipment on space missions. It has long been recognized that galactic cosmic rays are of such high energy that they tend to pass through available shielding materials resulting in exposure of astronauts and equipment within space vehicles and habitats. Any protection provided by shielding materials results not so much from stopping such particles but by changing their physical character by interaction with shielding material nuclei to hopefully less dangerous species. An understanding of these processes can be discerned by conducting various shielding simulations using the HZETRN computer code. Clearly, the fidelity of the nuclear cross sections are essential to correct specification of shield design and sensitivity of computational results to cross section error is important in guiding experimental validation of cross section models and the construction of cross section databases.

In this paper we examine a one-dimensional form of the Boltzmann transport equation (1), which is solved by way of the HZETRN code subject to the galactic cosmic rays and the 1977 solar minimum environment. The HZETRN code calculates a radiation dose equivalent, with units of (cSv/yr), associated with various depths within a shielding material. The radiation dose equivalent is a weighted sum of contributions from protons, alpha particles, light ions, medium ions, heavy ions and neutrons using the ICRP-60 LET dependent quality factor (ICRP, 1991). We consider production terms arising from 170 possible projectile-fragment cross-sections (Cucinotta, et al. 2003). The isotopes considered in the interactions are listed in the table 1. The accuracy of the resulting dose equivalent is dependent upon the

projectile-fragment production cross-sections. In the Boltzmann equation the stopping power and nuclear total cross sections are known to a high degree of accuracy but the fragmentation cross sections are more dependent upon details of the nuclear processes and consequently exhibit more uncertainty when tested experimentally (Wilson, et al. 1995, Golovchenko et al. 2002). We investigate the sensitivity of the dose equivalent calculations due to production cross section errors using sensitivity analysis. We do this error analysis for all possible projectile-fragment combinations (14,365) to estimate the sensitivity of the shielding calculations to errors introduced into a single nuclear fragmentation cross-section. Numerical differentiation with respect to the cross sections is evaluated for the selected shield materials of polyethylene, aluminum and copper. We will identify the most important cross sections affecting the dose equivalent calculations. The purpose of the investigation is to evaluate the cross sections impact on propagated errors in shielding estimates associated with radiation protection studies.

Error Analysis

We introduce a small error into a single projectile-fragment cross section on the right-hand side of equation (1) and calculate the error in the calculated dose equivalent. Note that only one selected cross section out of 14,365 projectile-fragment cross sections on the right-hand side of equation (1) is being changed to calculate a resultant error in the dose equivalent. The error in the dose equivalent is obtained from a truncated Taylor series expansion in the parameter space defined by the set of 14,365 cross-section parameters. For example, in the case Δx is small one can use the first order error approximation for the error as

$$error = f(x+\Delta x, y, z, ...) - f(x, y, z, ...) = \frac{\partial f}{\partial x}\Delta x \ .$$

The partial derivative term is taken as defining the sensitivity of the function f(x,y,z,…) in relation to changes in the single variable x. Here only a single cross section σ_{jk} on the right-hand side of equation (1) is perturbed at a time to maintain parameter independence. These parameters appear on the right-hand side of equation (1) which is the gain side of the Boltzmann equation. The total cross section σ_j and the stopping power $S_j(E)$ on the left-hand side of equation (1), representing loss terms, has not been changed since these values are well known. One should note that this would technically violate the conservation of flux in the Boltzmann equation. This violation already exists resulting from uncertainty of especially the fragmentation cross sections as known from experiments (for example, Golovchenko et al. 2002). This paper evaluates the gradient of dose equivalent with respect to the fragmentation cross section parameter space at the location of nominal cross section values so that the effects of off-nominal values can be further investigated. Adding terms to the left-hand side of equation (1) to maintain a conservation law would constrain the off-nominal domain to selected trajectories in parameter space where flux is

conserved. However, the relative importance of the dose equivalent errors, obtained by this research, would remain the same (especially within the parameter subspace where flux is conserved). Consequently, we have made the assumption that by changing consecutively only one projectile-fragment cross-section at a time, out of 14,365 cross sections occurring on the right-hand side of equation (1), the corresponding error in the total dose equivalent is small (crudely, 1 part in 14,365) and the cross term variations are of even higher order and negligible (similarly, 2 parts in 14,365). It should be further noted that the dose equivalent is a function of both energy and square of the charge of the ionizing radiation. It is proportional to the square of the charge of the nucleus. In the example given by $^{56}\text{Fe} \rightarrow {}^{55}\text{Mn+p}$, the dose deposited before the fragmentation occurs is proportional to $56^2=3136$, and after the fragmentation it is proportional to $55^2+1=3026$. So the energy deposit is 110/3026 times larger before the fragmentation than after. It is known that such fragmentation processes are used to reduce the radiation damage effects. In this example, we have not taken into account the energy effects because for the high energy processes that this paper discusses the energies of the initial ionizing ion are very comparable to the fragmenting nuclei.

We calculate the above Taylor series representation of the errors for each of all possible projectile-fragment combinations (14,365). These individual errors are then used to estimate the sensitivity of the shielding calculations to errors in all the nuclear fragmentation cross-sections. Numerical differentiation with respect to the cross sections is evaluated for the selected shield materials of polyethylene, aluminum and copper. We will identify the most important cross sections and corresponding ions for further experimental study. The purpose of the investigation is to evaluate the cross sections impact on propagated errors in shielding estimates associated with radiation protection studies.

Unitarity Considerations

We examine the role of unitarity in the evaluation of the sensitivity coefficients. We note that given a cross section data set $(\sigma_{jk}+\varepsilon_{jk})$ where ε_{jk} represents the uncertainty in cross section knowledge, there is no *a priori* prescription for satisfying unitarity and one uses arbitrary models. If we are to arbitrarily apply a unitarity requirement then the appropriate functionality is

$$H(\sigma_{jk}+\varepsilon_{jk}) \Rightarrow H[U(\sigma_{jk}+\varepsilon_{jk})] = H(\sigma_{jk}+\varepsilon_{jk}) + \sum H(\sigma_{lk}+\varepsilon_{lk}') \qquad (3)$$

where ε_{lk}' represents the modifications due to the chosen unitarity process denoted by the operator U and the sum extends over all l,k modified by the unitarity requirement. We will examine the relationship of variations of $H(\sigma_{jk}+\varepsilon_{jk})$ relative to variations in $H[U(\sigma_{jk}+\varepsilon_{jk})]$. This relationship is clarified by using the chain rule of partial differentiation. Hence, one can write

$$D_{\varepsilon_{jk}} H[U(\sigma_{jk} + \varepsilon_{jk})] = \frac{\partial H(\sigma_{jk} + \varepsilon_{jk})}{\partial \varepsilon_{jk}} + \sum [\frac{\partial H(\sigma_{lk} + \varepsilon_{lk}')}{\partial \varepsilon_{lk}'}] \frac{\partial \varepsilon_{lk}'}{\partial \varepsilon_{jk}} \qquad (4)$$

where D denotes a total derivative operator (both explicit and implicit differentials) and the sum extends over all parameters ε_{jk}' demanded by U. One form of unitarity is that any perturbation of a fragmentation cross section needs to be balanced by a change in the projectile absorption cross section σ_k as given by

$$\Sigma\, A_j\, (\sigma_{jk} + \varepsilon_{jk}) = A_k\, (\sigma_k + \varepsilon'_k) \qquad (5)$$

where the sum extends over all the j fragments and only one value of ε_{jk} is nonzero in that description. In this case, ε'_k is numerically $A_j\, \varepsilon_{jk}/A_k$. An alternate unitarity principle by Dr. J. Letaw from the literature, (Letaw 1985), is to assume the balance is made in the lightest fragment as

$$A_1\, (\sigma_{1k} + \varepsilon'_{1k}) + \Sigma\, A_j\, (\sigma_{jk} + \varepsilon_{jk}) = A_k\, \sigma_k \qquad (6)$$

where the sum extends over $j > 1$ and only one value of ε_{jk} is specified as nonzero but for arbitrary j greater than one. In this case, ε'_{1k} is numerically $-A_j\, \varepsilon_{jk}/A_1$. It is clear that any arbitrary form of normalization for mass conservation can be used resulting in a broad range of arbitrary results for the "constrained sensitivity coefficients." In any case, equation (5) is a poor choice as the absorption cross sections are accurately known for which the implied uncertainty factor ε'_k is misapplied. For a third alternate choice of renormalization of fragmentation models, that was used to improve comparisons with Ne beam experiments to conserve mass and charge, was applied equally to all fragments, see Wilson et al. (1991). We will now examine the impact of the two schemes of renormalization given by equations (5) and (6) on the sensitivity coefficients outcomes.

Aside from factors dependent on kinematic variables, depth, and intensity at the boundary, the contribution to dose equivalent resulting from a given k primary ion is approximately proportional to

$$H_k = \Sigma Q_j\, Z_j^2\, \sigma_{jk} + Q_k\, Z_k^2\, (1 - \sigma_k) \qquad (7)$$

where the sum is over all j and Q_j is a representative value of the quality factor. The total H is the sum over all j weighted by the k fluence at the boundary F_k. It is clear from equation (7) that the ε_{jk} sensitivity (explicit derivative of H), apart from weighting with the k ion fluence at the boundary, is

$$\frac{\partial H}{\partial \sigma_{jk}} = Q_j\, Z_j^2 \qquad (8)$$

where we note that this is a simple explicit partial derivative as appears in the Taylor expansion above. The sensitivity as argued by renormalization requirements needs added contributions from implicit differentials related to the constraints. Renormalization suggests requiring one to evaluate the total derivative consisting of explicit and implicit variations as

$$\left.\frac{\partial H}{\partial \sigma_{jk}}\right|_{total} = Q_j Z_j^2 - (A_j/A_k)\frac{\partial H}{\partial \sigma_j} = Q_j Z_j^2 - (A_j/A_k) Q_k Z_k^2 \qquad (9)$$

where A_j/A_k is the derivative of ε'_k with respect to ε_{jk} as required by equation (5). Note that the main contributions from j ion fragments will be for $Z_k \approx Z_j$ for which $A_k \approx A_j$ and the total derivative is near zero implying little sensitivity under this renormalization rule. There is no great mystery as to why this occurs. If one always balances the mass loss in a given ion by an ion of nearly equal charge and mass, the resulting change in H is quite small. Only those cross sections for which $Z_j << Z_k$ and $A_j << A_k$ will appear as important as shown by the analysis in equation (9) using constraint equation (5). Applying the same process to the Letaw renormalization of equation (6) one attains

$$\left.\frac{\partial H}{\partial \sigma_{jk}}\right|_{total} = Q_j Z_j^2 - (A_j/A_1)\frac{\partial H}{\partial \sigma_{1k}} = Q_j Z_j^2 - (A_j/A_1) Q_1 Z_1^2 . \qquad (10)$$

For the galactic cosmic ray HZE ions, $A_j \approx 2 Z_j$ and the Q_k is on the order of 20 to 30 while Q_1 is unity. It is clear that the derivative is large and nearly equal to the model independent sensitivity coefficient when $Z_k >> Z_1$ and near zero as $Z_k \Rightarrow Z_1$. What is clear from this simple analysis is that enforced different unitarity requirements introduces broad and conflicting results for the "sensitivity" as seen in the two examples above. The different choice of renormalization such as Letaw 's unitarity in equation (6) completely contradicts the choice of equation (5). Since the "unitarity requirement" is arbitrary and dependent on the choice of the unitarity renormalization scheme, we mainly focus on the unconstrained derivatives as best indicators of effects of cross section improvements. In all cases it is clear that the fundamental role is played by the sensitivity coefficients given by the explicit derivatives, but application of an arbitrary unitarity principle can lead to confusion in a final interpretation.

Unitarity is a constraint that can be implemented in an infinite number of different ways some of which can highly bias the results of a sensitivity analysis as previously discussed. We have compared the results obtained in this study, where unitarity is not fully enforced, with selected numerical experiments where a form of unitarity is imposed. The unitarity constraint imposed is based upon the fact that total absorption cross sections are known with much greater accuracy than partial fragmentation cross sections. Hence we selected a normalization constraint that keeps the total absorption cross section constant while only changing the fragmentation cross sections. Unitarity can then be enforced by introducing an error in one fragmentation cross section σ_{JK} while simultaneously lowering the cross sections σ_{Jk}, for k=J+1,…,170 and $k \neq K$. We lower these fragmentation cross sections by a constant factor in order that the sum $\sum_{k=j+1}^{170} \sigma_{jk}$ maintains its original value. We think that this method is less likely to introduce bias into

the calculation because the change in cross section is spread out equally throughout all the different fragmentation channels (similar to the Ne beam renormalization comparisons as shown by Wilson et al. 1991) rather than arbitrarily choosing a few channels to change. We then performed numerical experiments where the dose equivalent was calculated for errors in J,K values associated with the top 5 maximum errors listed in the table 3. The results from these selected numerical experiments was that the dose equivalent errors calculated with the imposed unitarity had the same values as previously obtained using our original calculations where renormalization was not used.

Taylor series approximation of Errors

Let H denote the total dose equivalent calculated by the HZETRN code using nominal cross sections from NUCFRG2 (Wilson et al. 1995). If a perturbation error $\varepsilon_{ij} > 0$ is introduced into a single fragmentation cross sections σ_{ij} used to calculate of the total dose equivalent, then what kind of errors can be expected in the predicted radiation dose equivalent? By employing a Taylor series expansion one can show that

$$\text{H}(\ \sigma_{ij} + \varepsilon_{ij}\ )\text{-H}(\ \sigma_{ij}\ ) = \sum_i \sum_j \frac{\partial H}{\partial \sigma_{ij}} \varepsilon_{ij} + \text{higher order terms.} \qquad (11)$$

Note that the matrix of partial derivatives on the right-hand side of equation (11) expresses the usual sensitivity of the dose equivalent H on the fragmentation cross section parameters σ_{ij}. We neglect the higher order terms of the Taylor series expansion and consider a single error associated with an i,j combination where i and j have fixed values. If the first order term is large, then the higher order terms would need to be examined. By introducing an error into a single cross section we can obtain a numerical approximation for just one term from the right-hand side of equation (5). By going through all i, j combinations one obtains a numerical approximation for each term on the right-hand side of the Taylor series. We can then use these numerical approximations for the derivatives to formulate a Monte Carlo simulation given by

$$H(\sigma_{ij} + \varepsilon_{ij}\eta_{ij}) = H(\sigma_{ij}) + \sum_i \sum_j \frac{\partial H}{\partial \sigma_{ij}} \varepsilon_{ij}\eta_{ij} \qquad (12)$$

where η_{ij} are random variates from a normal distribution In this way one can model the effect of errors in calculating the total dose equivalent.

The figure 1 illustrates the resulting Taylor series approximation for the errors in the dose equivalent at various depths within an aluminum shield due to the introduction of a single error in a specific k-projectile, j-fragment cross section without using any unitary considerations. For each given j,k value the

cross section σ_{jk} was replaced by $2\ \sigma_{jk}$ in order to control effects of round-off error. This was done for all 14,365 combinations of j and k. Also illustrated in the lower panel of these figures is the summation of fragment errors associated with a given projectile k. The figures 2 and 3 are similar figures for copper and polyethylene respectively.

Results and Discussion

Typical dose equivalent constituents are illustrated in the figures 5 and 6. The figures 1,2, and 3 illustrate the errors obtained in the dose equivalent calculations. These errors are a numerical representation of the derivative times the error representing a single term from the right-hand side of equation (9). The highest five peaks occurring in the figures 1,2 and 3, ordered from highest to lowest, correspond to the isotopes of $_{26}Fe^{56}$, $_{8}O^{16}$, $_{14}Si^{28}$, $_{12}Mg^{24}$ and $_{6}C^{12}$. These elements are the five most abundant heavier elements in the Galactic cosmic ray composition. The dose equivalent errors for aluminum, copper and polyethylene are more pronounced along the line of lower J-values and along the line where $j \approx k$. This is due to projectile interaction with shield material which causes few nucleon removal followed by resultant particle movement into the material showing up as the errors near the $j = k$ line. Consequently, the dose equivalent errors correspond to few nucleon removal followed by projectile fragment continuation after interaction.

Monte Carlo studies which incorporate errors from all sources were conducted by generating random values for η_{ij} from a normal distribution with mean $\mu = 0$, and standard deviation, std=0.75. We then conducted 50 Monte Carlo simulations for errors produced in the dose equivalent at various depths. Results from these simulations indicate low overall errors produced in the dose equivalent calculations. These results are indicated by the error bars on the curves given in figure 4. Also indicated in the figure 4 are curves obtained where all cross sections were set equal to zero. The tables 2,3 and 4 give the fifty maximum errors associated with 20 g/cm^2 of shield material for the materials of aluminum, polyethylene and copper respectively.

Similar sensitivity studies for an aluminum shield can be found by Townsend et al 1992, where in that study the production cross-sections σ_{jk} where replaced by $p\sigma_{jk}$, where p varied from 0.5 to 1.5 and the dose equivalent calculations where compared with the nominal values obtained when p=1.

One might conclude that the results of this study suggest that for the 1977 solar minimum environment and GCR environment, the dose equivalent is not very sensitive to errors in the production cross sections.

However, one can not conclude that secondary particle production is not important in general. Note that the production cross section errors can greatly affect the shielding requirements for a given dose limit. This is illustrated by the horizontal lines depicted in the figure 4. Particle production from lighter nucleon removal has the largest effect on dose equivalent from the HZETRN code. The largest change in dose equivalent is due to light, medium and heavy ion drop off with depth into shielding material. Emphasis on the most abundant elements in the Galactic cosmic rays and their particle interaction with the shield material is the most important issue in determining dose equivalent predictions. Future efforts are being directed toward developing additional physics and mathematics for describing the propagation of particles through a shielding medium.

Acknowledgement: This research was sponsored by NASA grant NAG-1-03075.

References

[1] J.W. Wilson, L.W. Townsend , W. Schimmerling, G.S. Khandalwal, F. Khan, J.E. Nealy, F.A. Cucinotta, L.C. Simonsen, J.L. Shinn, J.W. Norbury, Transport Methods and Interactions for Space Radiations, NASA Reference Publication-1257, (1991).

[**2**] F.A. Cucinotta, P.B. Sagonti, X.Hu, et al, Physics of the Isotope Dependence of Galactic Cosmic Ray Fluence Behind Shielding. NASA TP-2003-210792, 2003.

[3] J.L. Shinn, J.W. Wilson, An Efficient HZETRN (A Galactic Cosmic Ray Transport Code), NASA Technical Paper-3147, April, 1992.

[4] L.W. Townsend, F.A. Cucinotta, J.L. Shinn, J.W. Wilson, Effects of Fragmentation Parameter Variations on Estimates of Galactic Cosmic Ray Exposure-Dose Sensitivity Studies for Aluminum Shields , NASA Technical Memorandum-4386, July 1992.

[5] A.N. Golovchenko, J. Skvarc, N. Yasuda, M. Giacomelli, S.P. Trotyakova, R. Ilic, R. Bimbot, M. Toulemonde, T. Murakami, Total charge-changing and partial cross-section measurements in the reactions of ≈110-250 MeV/nucleon 12C in carbon, paraffin and in water. Phys. Rev.C 66:014609,2002.

[6] J. R. Letaw, Proton production cross sections in proton-nucleus collisions, Physical Review C, Vol. 28, No 5, November 1983.

[**7**] ICRP: 1990 Recommendations of the International Commission on Radiological Protection, ICRP Publication 60, 1991.

[**8**] Wilson, J.W., R.K. Tripathi, F.A. Cucinotta, J.L. Shinn, F.F. Badavi, S.Y. Chun, J.W. Norbury, C.J. Zeitlin, L.H. Hielbronn, J.Miller, NUCFRG2, An evaluation of the Semiempirical Nuclear Fragmentation Database, NASA TP-3533, 1995.

HZETRN Indices for Isotope Atomic Weight and Charge			
I	A	Z	Isotope
1	1	0	n
2	1	1	$_{1}H^{1}$
3	2	1	$_{1}H^{2}$
4	3	1	$_{1}H^{3}$
5	3	2	$_{2}He^{3}$
6	4	2	$_{2}He^{4}$
7	6	2	$_{2}He^{6}$
8	6	3	$_{3}Li^{6}$
9	7	3	$_{3}Li^{7}$
10	7	4	$_{4}Be^{7}$
11	8	3	$_{3}Li^{8}$
12	8	5	$_{5}B^{8}$
13	9	3	$_{3}Li^{9}$
14	9	4	$_{4}Be^{9}$
15	9	5	$_{5}B^{9}$
16	10	4	$_{4}Be^{10}$
17	10	5	$_{5}B^{10}$
18	10	6	$_{6}C^{10}$
19	11	4	$_{4}Be^{11}$
20	11	5	$_{5}B^{11}$
21	11	6	$_{6}C^{11}$
22	12	5	$_{5}B^{12}$
23	12	6	$_{6}C^{12}$
24	12	7	$_{7}N^{12}$
25	13	5	$_{5}B^{13}$
26	13	6	$_{6}C^{13}$
27	13	7	$_{7}N^{13}$
28	14	6	$_{6}C^{14}$
29	14	7	$_{7}N^{14}$
30	14	8	$_{8}O^{14}$
31	15	6	$_{6}C^{15}$
32	15	7	$_{7}N^{15}$
33	15	8	$_{8}O^{15}$
34	16	7	$_{7}N^{16}$
35	16	8	$_{8}O^{16}$
36	17	7	$_{7}N^{17}$
37	17	8	$_{8}O^{17}$
38	17	9	$_{9}F^{17}$
39	18	8	$_{8}O^{18}$
40	18	9	$_{9}O^{18}$
41	18	10	$_{10}Ne^{18}$
42	19	8	$_{8}O^{19}$
43	19	9	$_{9}F^{19}$
44	19	10	$_{10}Ne^{19}$
45	20	8	$_{8}O^{20}$
46	20	9	$_{9}F^{20}$
47	20	10	$_{10}Ne^{20}$
48	21	9	$_{9}F^{21}$
49	21	10	$_{10}Ne^{21}$
50	21	11	$_{11}Na^{21}$
51	22	10	$_{10}Ne^{22}$
52	22	11	$_{11}Na^{22}$
53	23	10	$_{10}Ne^{23}$
54	23	11	$_{11}Na^{23}$
55	23	12	$_{12}Mg^{23}$
56	24	10	$_{10}Ne^{24}$
57	24	11	$_{11}Na^{24}$

HZETRN Indices for Isotope Atomic Weight and Charge			
I	A	Z	Isotope
58	24	12	$_{12}Mg^{24}$
59	25	11	$_{11}Na^{25}$
60	25	12	$_{12}Mg^{25}$
61	25	13	$_{13}Al^{25}$
62	26	11	$_{11}Na^{26}$
63	26	12	$_{12}Mg^{26}$
64	26	13	$_{13}Al^{26}$
65	26	14	$_{14}Si^{26}$
66	27	12	$_{12}Mg^{27}$
67	27	13	$_{13}Al^{27}$
68	27	14	$_{14}Si^{27}$
69	28	12	$_{12}Mg^{28}$
70	28	13	$_{13}Al^{28}$
71	28	14	$_{14}Si^{28}$
72	29	13	$_{13}Al^{29}$
73	29	14	$_{14}Si^{29}$
74	29	15	$_{15}P^{29}$
75	30	13	$_{13}Al^{30}$
76	30	14	$_{14}Si^{30}$
77	30	15	$_{15}P^{30}$
78	30	16	$_{16}S^{30}$
79	31	14	$_{14}Si^{31}$
80	31	15	$_{15}P^{31}$
81	31	16	$_{16}S^{31}$
82	32	14	$_{14}Si^{32}$
83	32	15	$_{15}P^{32}$
84	32	16	$_{16}S^{32}$
85	33	14	$_{14}Si^{33}$
86	33	15	$_{15}P^{33}$
87	33	16	$_{16}S^{33}$
88	33	17	$_{17}Cl^{33}$
89	34	15	$_{15}P^{34}$
90	34	16	$_{16}S^{34}$
91	34	17	$_{17}Cl^{34}$
92	35	15	$_{15}P^{35}$
93	35	16	$_{16}S^{35}$
94	35	17	$_{17}Cl^{35}$
95	35	18	$_{18}Ar^{35}$
96	36	16	$_{16}S^{36}$
97	36	17	$_{17}Cl^{36}$
98	36	18	$_{18}Ar^{36}$
99	37	16	$_{16}S^{37}$
100	37	17	$_{17}Cl^{37}$
101	37	18	$_{18}Ar^{37}$
102	37	19	$_{19}K^{37}$
103	38	16	$_{16}S^{38}$
104	38	17	$_{17}Cl^{38}$
105	38	18	$_{18}Ar^{38}$
106	38	19	$_{19}K^{38}$
107	38	20	$_{20}Ca^{38}$
108	39	17	$_{17}Cl^{39}$
109	39	18	$_{18}Ar^{39}$
110	39	19	$_{19}K^{39}$
111	39	20	$_{20}Ca^{39}$
112	40	18	$_{18}Ar^{40}$
113	40	19	$_{19}K^{40}$
114	40	20	$_{20}Ca^{40}$

HZETRN Indices for Isotope Atomic Weight and Charge			
I	A	Z	Isotope
115	41	18	$_{18}Ar^{41}$
116	41	19	$_{19}K^{41}$
117	41	20	$_{20}Ca^{41}$
118	42	18	$_{18}Ar^{42}$
119	42	19	$_{19}K^{42}$
120	42	20	$_{20}Ca^{42}$
121	42	21	$_{21}Sc^{42}$
122	43	19	$_{19}K^{43}$
123	43	20	$_{20}Ca^{43}$
124	43	21	$_{21}Sc^{43}$
125	44	20	$_{20}Ca^{44}$
126	44	21	$_{21}Sc^{44}$
127	44	22	$_{22}Ti^{44}$
128	45	20	$_{20}Ca^{45}$
129	45	21	$_{21}Sc^{45}$
130	45	22	$_{22}Ti^{45}$
131	46	20	$_{20}Ca^{46}$
132	46	21	$_{21}Sc^{46}$
133	46	22	$_{22}Ti^{46}$
134	46	23	$_{23}V^{46}$
135	47	21	$_{21}Sc^{47}$
136	47	22	$_{22}Ti^{47}$
137	47	23	$_{23}V^{47}$
138	48	21	$_{21}Sc^{48}$
139	48	22	$_{22}Ti^{48}$
140	48	23	$_{23}V^{48}$
141	48	24	$_{24}Cr^{48}$
142	49	22	$_{22}Ti^{49}$
143	49	23	$_{23}V^{49}$
144	49	24	$_{24}Cr^{49}$
145	50	22	$_{22}Ti^{50}$
146	50	23	$_{23}V^{50}$
147	50	24	$_{24}Cr^{50}$
148	50	25	$_{25}Mn^{50}$
149	51	23	$_{23}V^{51}$
150	51	24	$_{24}Cr^{51}$
151	51	25	$_{25}Mn^{51}$
152	52	23	$_{23}V^{52}$
153	52	24	$_{24}Cr^{52}$
154	52	25	$_{25}Mn^{52}$
155	53	24	$_{24}Cr^{53}$
156	53	25	$_{25}Mn^{53}$
157	53	26	$_{26}Fe^{53}$
158	54	24	$_{24}Cr^{54}$
159	54	25	$_{25}Mn^{54}$
160	54	26	$_{26}Fe^{54}$
161	55	25	$_{25}Mn^{55}$
162	55	26	$_{26}Fe^{55}$
163	55	27	$_{27}Co^{55}$
164	56	26	$_{26}Fe^{56}$
165	56	27	$_{27}Co^{56}$
166	56	28	$_{28}Ni^{56}$
167	57	26	$_{26}Fe^{57}$
168	57	27	$_{27}CO^{57}$
169	57	28	$_{28}Ni^{57}$
170	58	28	$_{28}Ni^{58}$

Table 1. Projectile-fragmentation isotopes

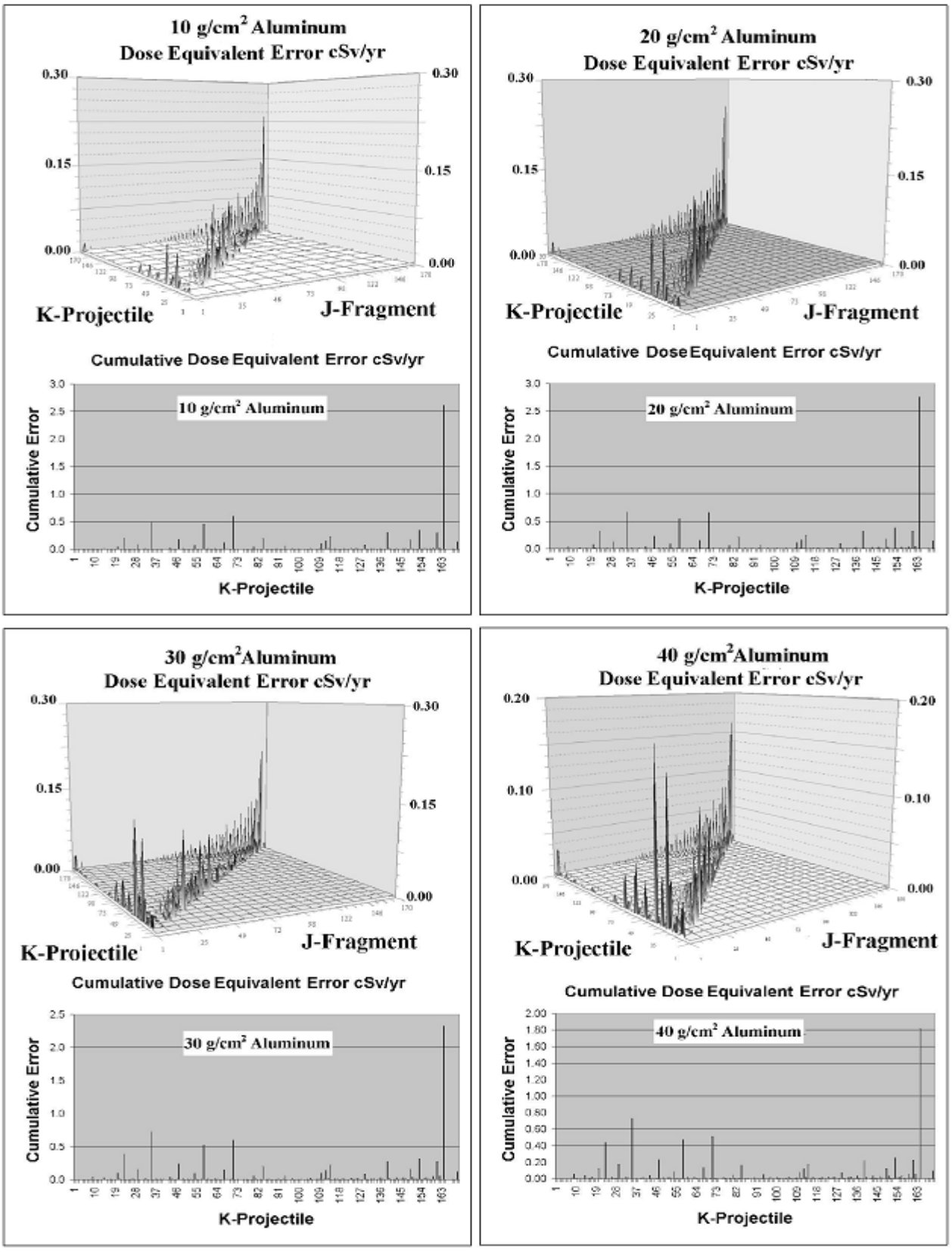

Figure 1. Error and cumulative error graphs for Aluminum shield at various depths

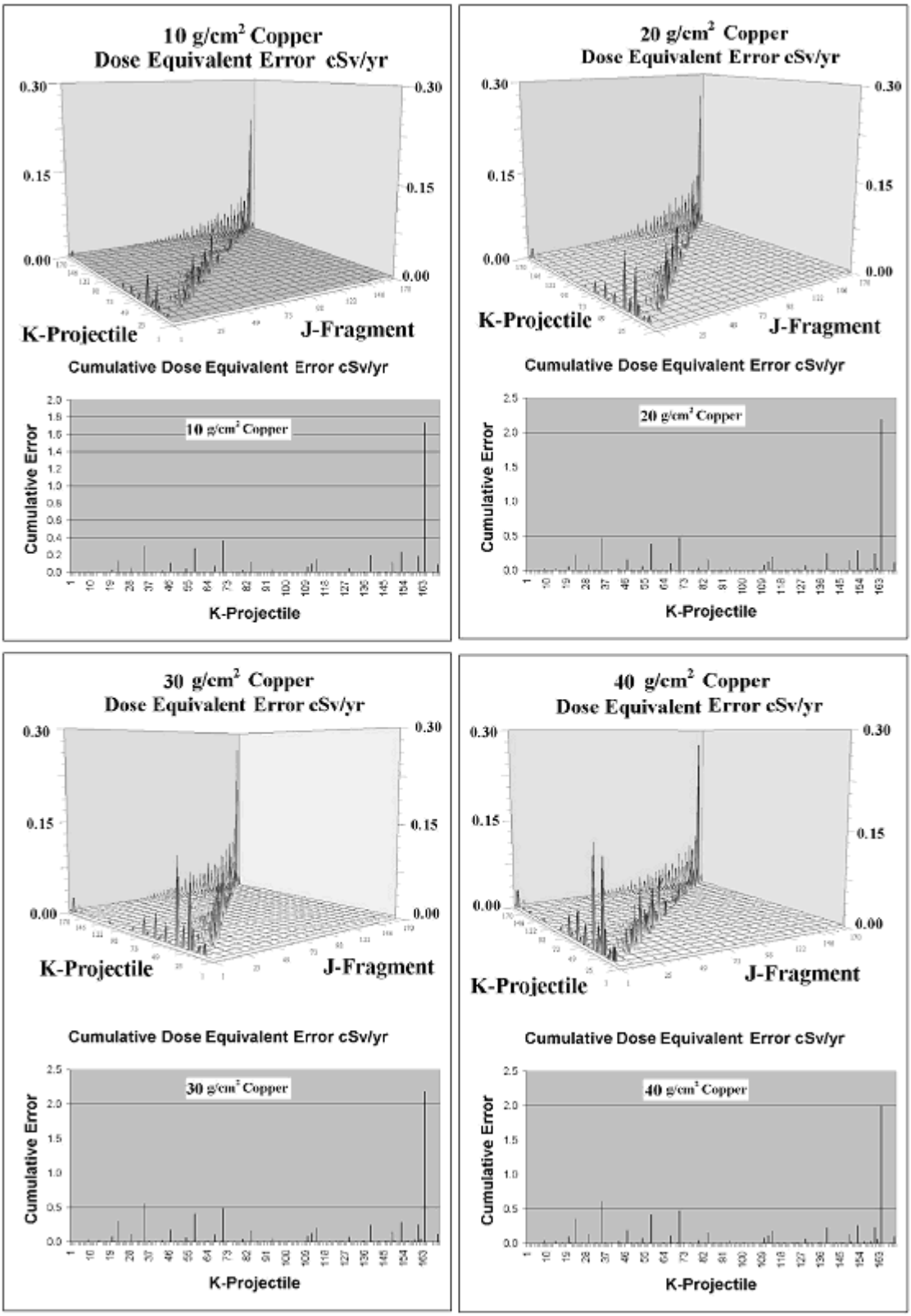

Figure 2. Error and cumulative error graphs for Copper shield at various depths

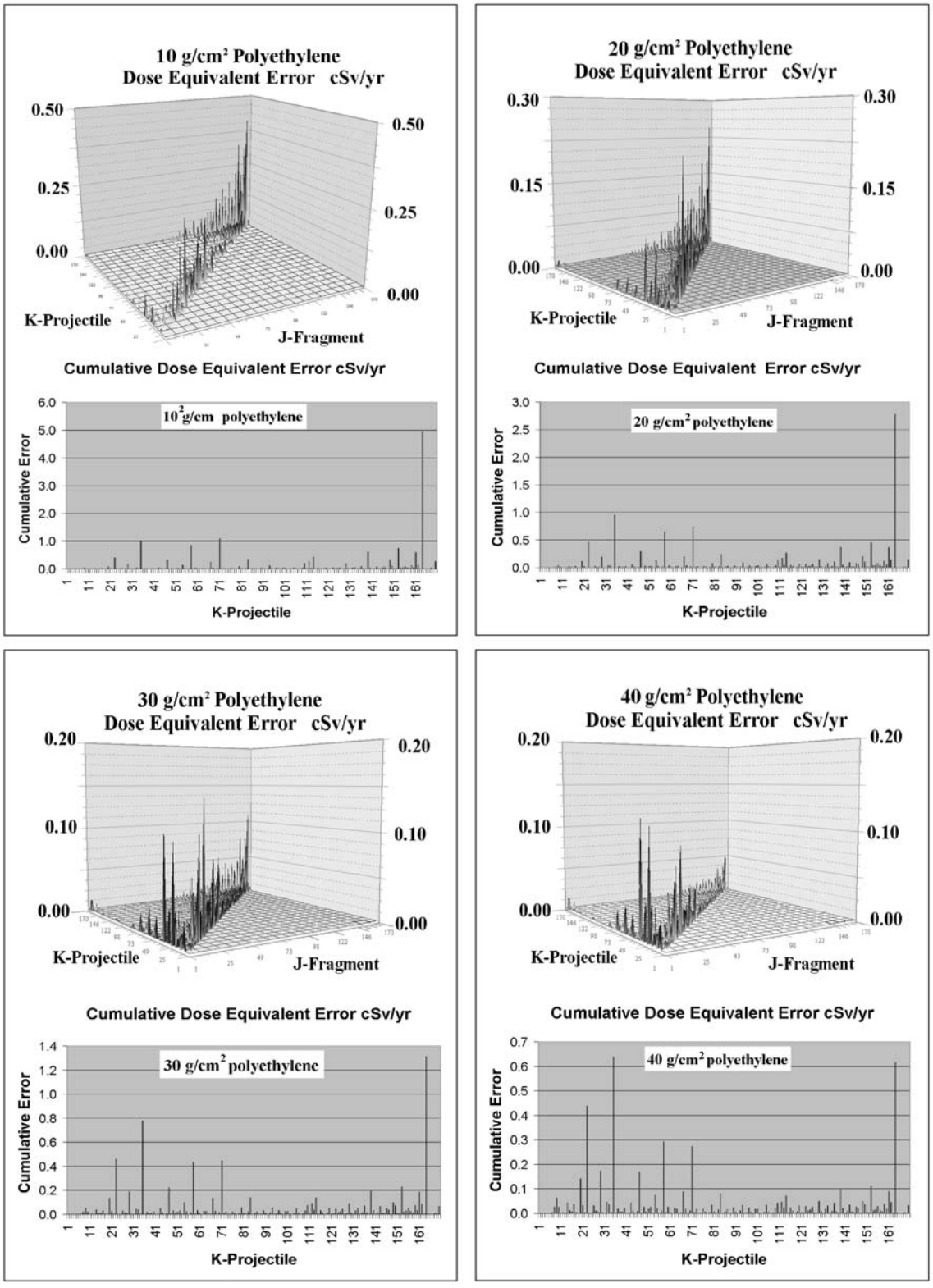

Figure 3. Error and cumulative error graphs for polyethylene shield at various depths

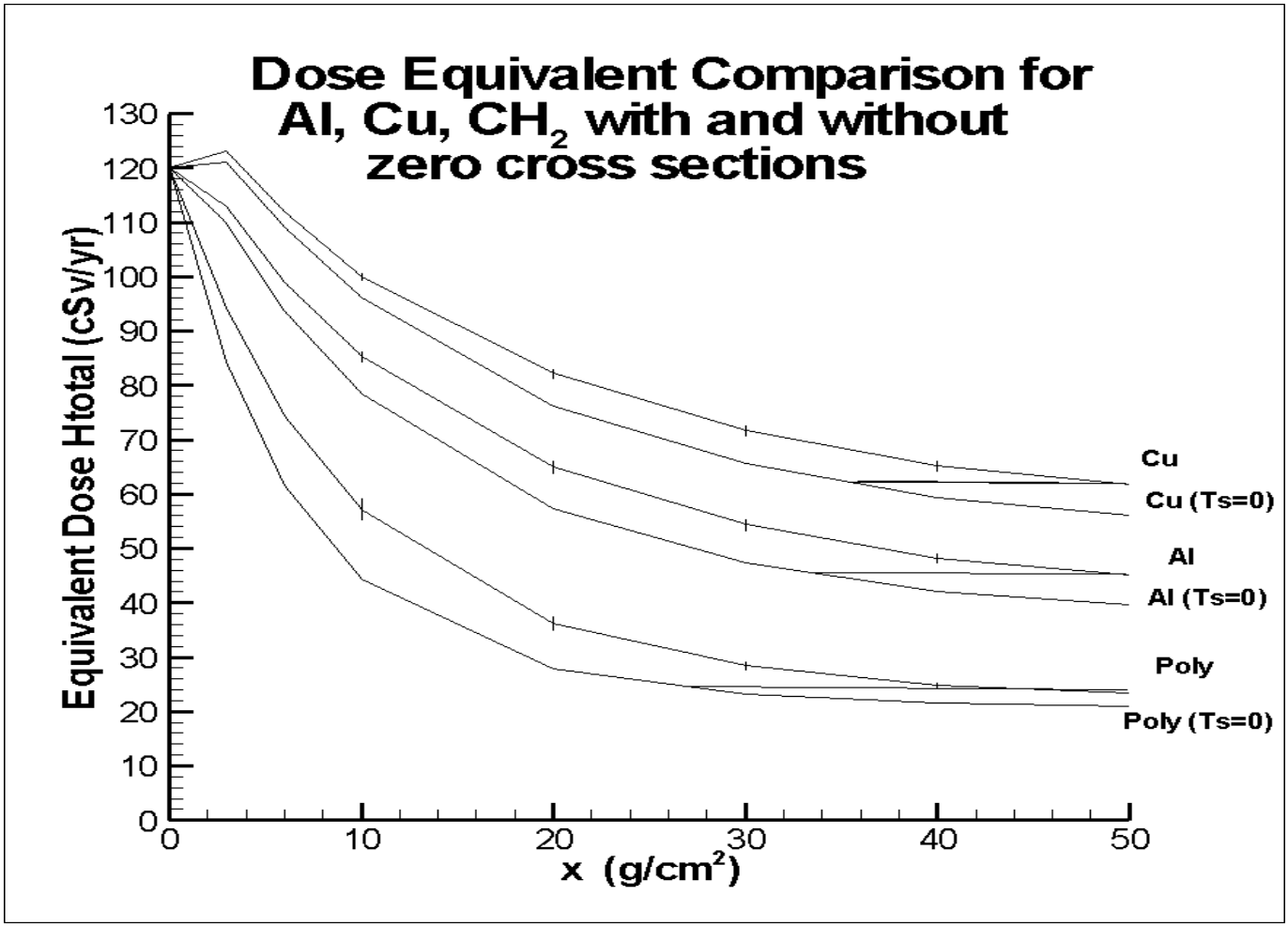

Figure 4. Dose equivalent comparison with and without production cross-sections equal to zero.

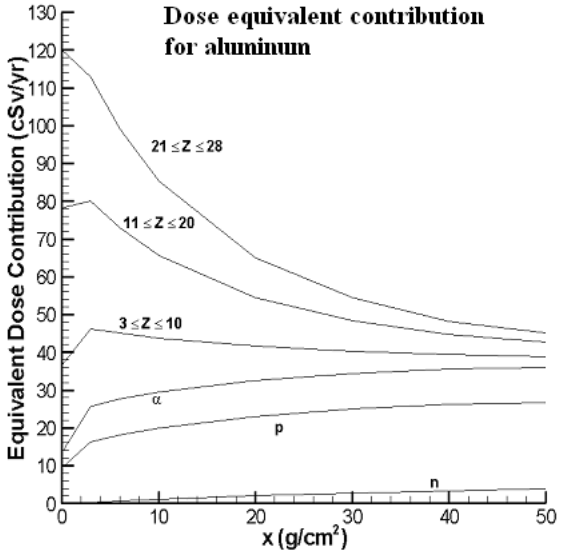

Figure 5.
Dose contribution Aluminum

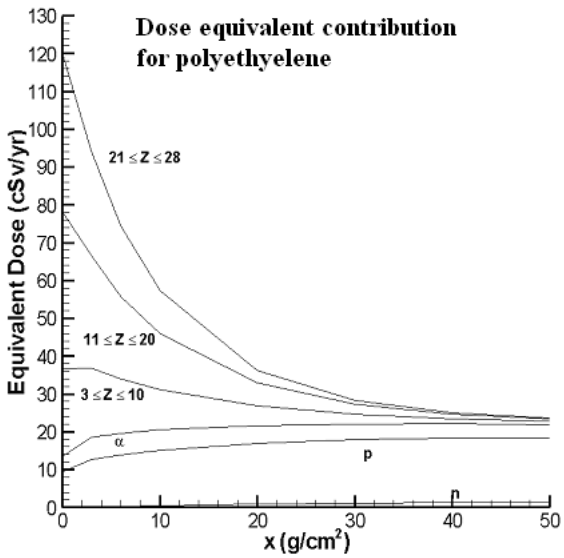

Figure 6.
Dose contribution polyethyelene

Range	J	K	Error	Fragment	Projectile		Range	J	K	Error	Fragment	Projectile
1	162	164	2.52E-01	$_{26}Fe^{55}$	$_{26}Fe^{56}$		26	123	164	5.55E-02	$_{20}Ca^{43}$	$_{26}Fe^{56}$
2	161	164	2.09E-01	$_{25}Mn^{55}$	$_{26}Fe^{56}$		27	133	164	5.46E-02	$_{22}Ti^{46}$	$_{26}Fe^{56}$
3	159	164	1.89E-01	$_{25}Mn^{54}$	$_{26}Fe^{56}$		28	126	164	5.39E-02	$_{21}Sc^{44}$	$_{26}Fe^{56}$
4	156	164	1.33E-01	$_{25}Mn^{53}$	$_{26}Fe^{56}$		29	21	23	5.31E-02	$_{6}C^{11}$	$_{6}C^{12}$
5	33	35	1.29E-01	$_{8}O^{15}$	$_{8}O^{16}$		30	49	58	5.09E-02	$_{10}Ne^{21}$	$_{12}Mg^{24}$
6	153	164	1.21E-01	$_{24}Cr^{52}$	$_{26}Fe^{56}$		31	140	164	5.06E-02	$_{23}V^{48}$	$_{26}Fe^{56}$
7	150	164	1.12E-01	$_{24}Cr^{51}$	$_{26}Fe^{56}$		32	120	164	5.02E-02	$_{20}Ca^{42}$	$_{26}Fe^{56}$
8	2	35	1.11E-01	$_{1}H^{1}$	$_{8}O^{16}$		33	52	58	4.80E-02	$_{11}Na^{22}$	$_{12}Mg^{24}$
9	68	71	1.07E-01	$_{14}Si^{27}$	$_{14}Si^{28}$		34	147	164	4.59E-02	$_{24}Cr^{50}$	$_{26}Fe^{56}$
10	143	164	9.86E-02	$_{23}V^{49}$	$_{26}Fe^{56}$		35	113	164	4.45E-02	$_{19}K^{40}$	$_{26}Fe^{56}$
11	55	58	9.57E-02	$_{12}Mg^{23}$	$_{12}Mg^{24}$		36	160	164	4.37E-02	$_{26}Fe^{54}$	$_{26}Fe^{56}$
12	2	23	9.51E-02	$_{1}H^{1}$	$_{6}C^{12}$		37	26	35	4.35E-02	$_{6}C^{13}$	$_{8}O^{16}$
13	67	71	9.18E-02	$_{13}Al^{27}$	$_{14}Si^{28}$		38	44	47	4.34E-02	$_{10}Ne^{19}$	$_{10}Ne^{20}$
14	29	35	8.83E-02	$_{7}N^{14}$	$_{8}O^{16}$		39	154	164	4.22E-02	$_{25}Mn^{52}$	$_{26}Fe^{56}$
15	136	164	8.65E-02	$_{22}Ti^{47}$	$_{26}Fe^{56}$		40	116	164	4.16E-02	$_{9}O^{18}$	$_{26}Fe^{56}$
16	146	164	8.58E-02	$_{23}V^{50}$	$_{26}Fe^{56}$		41	132	164	4.04E-02	$_{21}Sc^{46}$	$_{26}Fe^{56}$
17	32	35	8.17E-02	$_{7}N^{15}$	$_{8}O^{16}$		42	23	35	3.85E-02	$_{6}C^{12}$	$_{8}O^{16}$
18	54	58	7.60E-02	$_{11}Na^{23}$	$_{12}Mg^{24}$		43	105	164	3.81E-02	$_{18}Ar^{38}$	$_{26}Fe^{56}$
19	129	164	7.05E-02	$_{21}Sc^{45}$	$_{26}Fe^{56}$		44	54	71	3.77E-02	$_{11}Na^{23}$	$_{14}Si^{28}$
20	1	35	6.97E-02	n	$_{8}O^{16}$		45	64	71	3.65E-02	$_{13}Al^{26}$	$_{14}Si^{28}$
21	60	71	6.28E-02	$_{12}Mg^{25}$	$_{14}Si^{28}$		46	17	23	3.64E-02	$_{5}B^{10}$	$_{6}C^{12}$
22	139	164	6.11E-02	$_{22}Ti^{48}$	$_{26}Fe^{56}$		47	150	153	3.58E-02	$_{24}Cr^{51}$	$_{24}Cr^{52}$
23	1	23	5.97E-02	n	$_{6}C^{12}$		48	111	114	3.44E-02	$_{20}Ca^{39}$	$_{20}Ca^{40}$
24	155	164	5.90E-02	$_{24}Cr^{53}$	$_{26}Fe^{56}$		49	136	139	3.40E-02	$_{22}Ti^{47}$	$_{22}Ti^{47}$
25	63	71	5.85E-02	$_{12}Mg^{26}$	$_{14}Si^{28}$		50	51	58	3.39E-02	$_{10}Ne^{22}$	$_{12}Mg^{24}$

Table 2. Dose equivalent sensitivity with top 50 cross sections
Maximum errors (cSv/yr) associated with 20 g/cm^2 of aluminum shield.

Range	J	K	Error	Fragment	Projectile		Range	J	K	Error	Fragment	Projectile
1	162	164	2.51E-01	$_{26}Fe^{55}$	$_{26}Fe^{56}$		26	157	164	6.65E-02	$_{26}Fe^{53}$	$_{26}Fe^{56}$
2	33	35	2.06E-01	$_{8}O^{15}$	$_{8}O^{16}$		27	155	164	6.59E-02	$_{24}Cr^{53}$	$_{26}Fe^{56}$
3	159	164	1.82E-01	$_{25}Mn^{54}$	$_{26}Fe^{56}$		28	133	164	6.49E-02	$_{22}Ti^{46}$	$_{26}Fe^{56}$
4	161	164	1.76E-01	$_{25}Mn^{55}$	$_{26}Fe^{56}$		29	147	164	6.01E-02	$_{24}Cr^{50}$	$_{26}Fe^{56}$
5	153	164	1.68E-01	$_{24}Cr^{52}$	$_{26}Fe^{56}$		30	17	23	5.78E-02	$_{5}B^{10}$	$_{6}C^{12}$
6	29	35	1.54E-01	$_{7}N^{14}$	$_{8}O^{16}$		31	20	23	5.70E-02	$_{5}B^{11}$	$_{6}C^{12}$
7	55	58	1.32E-01	$_{12}Mg^{23}$	$_{12}Mg^{24}$		32	26	35	5.61E-02	$_{6}C^{13}$	$_{8}O^{16}$
8	68	71	1.30E-01	$_{14}Si^{27}$	$_{14}Si^{28}$		33	64	71	5.48E-02	$_{13}Al^{26}$	$_{14}Si^{28}$
9	32	35	1.27E-01	$_{7}N^{15}$	$_{8}O^{16}$		34	120	164	5.43E-02	$_{20}Ca^{42}$	$_{26}Fe^{56}$
10	150	164	1.27E-01	$_{24}Cr^{51}$	$_{26}Fe^{56}$		35	49	58	5.39E-02	$_{10}Ne^{21}$	$_{12}Mg^{24}$
11	156	164	1.14E-01	$_{25}Mn^{53}$	$_{26}Fe^{56}$		36	63	71	5.33E-02	$_{12}Mg^{26}$	$_{14}Si^{28}$
12	143	164	1.11E-01	$_{23}V^{49}$	$_{26}Fe^{56}$		37	123	164	5.23E-02	$_{20}Ca^{43}$	$_{26}Fe^{56}$
13	21	23	1.05E-01	$_{6}C^{11}$	$_{6}C^{12}$		38	44	47	5.17E-02	$_{10}Ne^{19}$	$_{10}Ne^{20}$
14	2	35	9.97E-02	$_{1}H^{1}$	$_{8}O^{16}$		39	1	35	5.02E-02	n	$_{8}O^{16}$
15	136	164	9.92E-02	$_{22}Ti^{47}$	$_{26}Fe^{56}$		40	140	164	4.91E-02	$_{23}V^{48}$	$_{26}Fe^{56}$
16	67	71	9.13E-02	$_{13}Al^{27}$	$_{14}Si^{28}$		41	126	164	4.85E-02	$_{21}Sc^{44}$	$_{26}Fe^{56}$
17	160	164	9.03E-02	$_{26}Fe^{54}$	$_{26}Fe^{56}$		42	47	58	4.58E-02	$_{10}Ne^{20}$	$_{12}Mg^{24}$
18	2	23	8.67E-02	$_{1}H^{1}$	$_{6}C^{12}$		43	154	164	4.57E-02	$_{25}Mn^{52}$	$_{26}Fe^{56}$
19	54	58	8.39E-02	$_{11}Na^{23}$	$_{12}Mg^{24}$		44	58	71	4.55E-02	$_{12}Mg^{24}$	$_{14}Si^{28}$
20	23	35	8.37E-02	$_{6}C^{12}$	$_{8}O^{16}$		45	150	153	4.32E-02	$_{24}Cr^{51}$	$_{24}Cr^{52}$
21	139	164	7.76E-02	$_{22}Ti^{48}$	$_{26}Fe^{56}$		46	1	23	4.30E-02	n	$_{6}C^{12}$
22	129	164	7.75E-02	$_{21}Sc^{45}$	$_{26}Fe^{56}$		47	23	29	4.13E-02	$_{6}C^{12}$	$_{7}N^{14}$
23	146	164	7.17E-02	$_{23}V^{50}$	$_{26}Fe^{56}$		48	43	47	3.91E-02	$_{9}F^{19}$	$_{10}Ne^{20}$
24	52	58	7.05E-02	$_{11}Na^{22}$	$_{12}Mg^{24}$		49	136	139	3.88E-02	$_{22}Ti^{47}$	$_{22}Ti^{48}$
25	60	71	6.86E-02	$_{12}Mg^{25}$	$_{14}Si^{28}$		50	81	84	3.81E-02	$_{16}S^{31}$	$_{16}S^{32}$

Table 3. Dose equivalent sensitivity with top 50 cross sections
Maximum errors (cSv/yr) associated with 20 g/cm^2 of polyethylene shield.

Rank	J	K	Error	Fragment	Projectile		Rank	J	K	Error	Fragment	Projectile
1	162	164	2.90E-01	$_{26}Fe^{55}$	$_{26}Fe^{56}$		26	133	164	4.09E-02	$_{22}Ti^{46}$	$_{26}Fe^{56}$
2	161	164	1.87E-01	$_{25}Mn^{55}$	$_{26}Fe^{56}$		27	126	164	4.08E-02	$_{21}Sc^{44}$	$_{26}Fe^{56}$
3	159	164	1.32E-01	$_{25}Mn^{54}$	$_{26}Fe^{56}$		28	63	71	3.90E-02	$_{12}Mg^{26}$	$_{14}Si^{28}$
4	156	164	9.42E-02	$_{25}Mn^{53}$	$_{26}Fe^{56}$		29	120	164	3.86E-02	$_{20}Ca^{42}$	$_{26}Fe^{56}$
5	2	35	8.84E-02	$_{1}H^{1}$	$_{8}O^{16}$		30	140	164	3.75E-02	$_{23}V^{48}$	$_{26}Fe^{56}$
6	153	164	8.67E-02	$_{24}Cr^{52}$	$_{26}Fe^{56}$		31	150	153	3.73E-02	$_{24}Cr^{51}$	$_{24}Cr^{52}$
7	33	35	8.51E-02	$_{11}Na^{22}$	$_{8}O^{16}$		32	113	164	3.45E-02	$_{19}K^{40}$	$_{26}Fe^{56}$
8	150	164	8.11E-02	$_{24}Cr^{51}$	$_{26}Fe^{56}$		33	136	139	3.37E-02	$_{22}Ti^{47}$	$_{22}Ti^{48}$
9	68	71	7.86E-02	$_{14}Si^{27}$	$_{14}Si^{28}$		34	21	23	3.37E-02	$_{6}C^{11}$	$_{6}C^{12}$
10	2	23	7.66E-02	$_{1}H^{1}$	$_{6}C^{12}$		35	49	58	3.34E-02	$_{10}Ne^{21}$	$_{12}Mg^{24}$
11	67	71	7.24E-02	$_{13}Al^{27}$	$_{14}Si^{28}$		36	147	164	3.34E-02	$_{24}Cr^{50}$	$_{26}Fe^{56}$
12	143	164	7.24E-02	$_{23}V^{49}$	$_{26}Fe^{56}$		37	116	164	3.19E-02	$_{19}K^{41}$	$_{26}Fe^{56}$
13	55	58	6.70E-02	$_{12}Mg^{23}$	$_{12}Mg^{24}$		38	111	114	3.19E-02	$_{20}Ca^{39}$	$_{20}Ca^{40}$
14	136	164	6.45E-02	$_{22}Ti^{47}$	$_{26}Fe^{56}$		39	52	58	3.14E-02	$_{11}Na^{22}$	$_{12}Mg^{24}$
15	146	164	6.22E-02	$_{23}V^{50}$	$_{26}Fe^{56}$		40	160	164	3.07E-02	$_{26}Fe^{54}$	$_{26}Fe^{56}$
16	1	35	5.76E-02	n	$_{8}O^{16}$		41	159	161	3.05E-02	$_{25}Mn^{54}$	$_{25}Mn^{55}$
17	29	35	5.65E-02	$_{7}N^{14}$	$_{8}O^{16}$		42	154	164	3.04E-02	$_{25}Mn^{52}$	$_{26}Fe^{56}$
18	54	58	5.65E-02	$_{11}Na^{23}$	$_{12}Mg^{24}$		43	132	164	3.01E-02	$_{21}Sc^{46}$	$_{26}Fe^{56}$
19	32	35	5.38E-02	$_{7}N^{15}$	$_{8}O^{16}$		44	105	164	2.97E-02	$_{18}Ar^{38}$	$_{26}Fe^{56}$
20	129	164	5.33E-02	$_{21}Sc^{45}$	$_{26}Fe^{56}$		45	44	47	2.85E-02	$_{10}Ne^{19}$	$_{10}Ne^{20}$
21	1	23	5.05E-02	n	$_{6}C^{12}$		46	2	58	2.83E-02	$_{1}H^{1}$	$_{12}Mg^{24}$
22	139	164	4.50E-02	$_{22}Ti^{48}$	$_{26}Fe^{56}$		47	26	35	2.78E-02	$_{6}C^{13}$	$_{8}O^{16}$
23	60	71	4.24E-02	$_{12}Mg^{25}$	$_{14}Si^{28}$		48	149	153	2.70E-02	$_{23}V^{51}$	$_{24}Cr^{52}$
24	123	164	4.21E-02	$_{20}Ca^{43}$	$_{26}Fe^{56}$		49	81	84	2.62E-02	$_{16}S^{31}$	$_{16}S^{32}$
25	155	164	4.17E-02	$_{24}Cr^{53}$	$_{26}Fe^{56}$		50	54	71	2.57E-02	$_{11}Na^{23}$	$_{14}Si^{28}$

Table 4. Dose equivalent sensitivity with top 50 cross sections
Maximum errors (cSv/yr) associated 20 g/cm^2 copper shield.

REPORT DOCUMENTATION PAGE

Form Approved
OMB No. 0704-0188

1. REPORT DATE *(DD-MM-YYYY)*	2. REPORT TYPE	3. DATES COVERED *(From - To)*
01- 12 - 2005	Technical Publication	

4. TITLE AND SUBTITLE

Cross Section Sensitivity and Propagated Errors in HZE Exposures

5a. CONTRACT NUMBER

5b. GRANT NUMBER

5c. PROGRAM ELEMENT NUMBER

6. AUTHOR(S)

Heinbockel, John H.; Wilson, John W.; Blattnig, Steve R.;
Qualls, Garry D.; Badavi, Francis F.; and Cucinotta, Francis A.

5d. PROJECT NUMBER

5e. TASK NUMBER

5f. WORK UNIT NUMBER

23-101-15-10

7. PERFORMING ORGANIZATION NAME(S) AND ADDRESS(ES)

NASA Langley Research Center
Hampton, VA 23681-2199

8. PERFORMING ORGANIZATION REPORT NUMBER

L-19085

9. SPONSORING/MONITORING AGENCY NAME(S) AND ADDRESS(ES)

National Aeronautics and Space Administration
Washington, DC 20546-0001

10. SPONSOR/MONITOR'S ACRONYM(S)

NASA

11. SPONSOR/MONITOR'S REPORT NUMBER(S)

NASA/TP-2005-213945

12. DISTRIBUTION/AVAILABILITY STATEMENT

Unclassified - Unlimited
Subject Category 92
Availability: NASA CASI (301) 621-0390

13. SUPPLEMENTARY NOTES

An electronic version can be found at http://ntrs.nasa.gov

14. ABSTRACT

It has long been recognized that galactic cosmic rays are of such high energy that they tend to pass through available shielding materials resulting in exposure of astronauts and equipment within space vehicles and habitats. Any protection provided by shielding materials result not so much from stopping such particles but by changing their physical character in interaction with shielding material nuclei forming, hopefully, less dangerous species. Clearly, the fidelity of the nuclear cross-sections is essential to correct specification of shield design and sensitivity to cross-section error is important in guiding experimental validation of cross-section models and database. We examine the Boltzmann transport equation which is used to calculate dose equivalent during solar minimum, with units (cSv/yr), associated with various depths of shielding materials. The dose equivalent is a weighted sum of contributions from neutrons, protons, light ions, medium ions and heavy ions. We investigate the sensitivity of dose equivalent calculations due to errors in nuclear fragmentation cross-sections.

15. SUBJECT TERMS

Radiation shielding; Cross section errors; Unitarity; Sensitivity; HZETRN; Dose equivalent

16. SECURITY CLASSIFICATION OF:			17. LIMITATION OF ABSTRACT	18. NUMBER OF PAGES	19a. NAME OF RESPONSIBLE PERSON
a. REPORT	b. ABSTRACT	c. THIS PAGE			STI Help Desk (email: help@sti.nasa.gov)
					19b. TELEPHONE NUMBER *(Include area code)*
U	U	U	UU	22	(301) 621-0390